Supplementary Information: Electronic structure and optical properties of halide double perovskites from a Wannier-localized optimally-tuned, screened range-separated hybrid functional

Francisca Sagredo,[1,2] Stephen E. Gant,[1,2] Guy Ohad,[3] Jonah B. Haber,[1,2] Marina R. Filip,[4] Leeor Kronik,[3] and Jeffrey B. Neaton[1,2]

[1] *Material Science Division, Lawrence Berkeley National Lab, Berkeley, CA 94720*
[2] *Department of Physics, University of California, Berkeley, California 94720, USA*
[3] *Department of Molecular Chemistry and Materials Science, Weizmann Institute of Science, Rehovoth 76100, Israel*
[4] *Department of Physics, University of Oxford, Oxford OX1 3PJ, United Kingdom*

(Dated: December 13, 2024)

I. COMPUTATIONAL DETAILS

A. DFT details

The dielectric constants needed for step 1 of the WOT-SRSH procedure (see Sec II of main text) for the Bi and Sb compounds are taken from Ref. [1] where they were obtained from the inverse of the head of RPA dielectric function computed using the epsilon code in the `BerkeleyGW` [2–4] software package. The dielectric constant for $Cs_2AgTlBr_6$ is computed here in the same manner. We use the optimized norm-conserving fully relativistic pseudopotentials available from the PSEUDO-DOJO repository [5] for all calculations. In Table I, we show the electron configurations of all pseudopotentials used. All calculations with Cs, Ag, Bi, Sb, and Tl explicitly include a full shell of semicore electrons. For Cl only the outermost $n = 3$ electrons are considered explicitly. For Br, only the outermost $n = 4$ electrons are considered explicitly for all DFT-only calculations, while for all G_0W_0 calculations the $n = 3$ shell of semi-core electrons is also explicitly considered. This is done to minimize computational cost and to avoid errors which can arise when only a fraction of the electrons of a principal quantum number are considered explicitly [6–10]. We also observe that at the DFT level, the difference in the electronic band gap between these two Br pseudos is negligible, but for *GW* calculations these additional states have been shown to affect band gap results [10] which is why they are used.

The Perdew-Burke-Erzenhof (PBE) [11] functional is used for all of the initial Wannierization calculations, with the exception of PBE0 [12], which is used for the thallium compound in step 1. This is due to a known issue where PBE incorrectly predicts $Cs_2AgTlBr_6$ to not have a gap [13]. The `WANNIER90` package [14] is used in step 2. All calculations from step 2-4 are done using a modified version of the `QUANTUM ESPRESSO` plane wave code [15–17]. $2\times2\times2$ supercells of the primitive unit cell are used for steps 2 and 3. As in the previously reported results [18], Γ-point only k-point grid calculations were used, with a cut off energy of 70 Ry. The Makov-Payne image charge correction is used to correct the energy of the $N-1$ electron as stated in the main text. Finally, in step 4 we use a $4\times4\times4$ k-grid with a plane wave cutoff of 70 Ry. Spin-orbit coupling (SOC) effects are included in the final calculation in step 4, but are neglected in the Wannierization procedure of step 1.

Element	Valence e Config.
Cs	$6s^1 5p^6 5s^2$
Ag	$5s^1 4d^{10} 4p^6 4s^2$
Bi	$6p^3 6s^2 5d^{10} 5p^6 5s^2$
Sb	$5p^3 5s^2 4d^{10} 4p^6 4s^2$
Tl	$6p^1 6s^2 5d^{10} 5p^6 5s^2$
Cl	$3p^5 3s^2$
Br	$4p^5 4s^2 3d^{10} 3p^6 3s^2$ $4p^5 4s^2$

TABLE I. Valence electron configurations used for the pseudopotentials for each element. Two configurations are provided for Br,with the first used in *GW* calculations and the second in the DFT-only calculations.

B. TDDFT

Linear response time-dependent DFT (TDDFT) calculations are performed with the Vienna *ab initio* simulation package (VASP)[19] using the PBE-based projector augmented wave method for treating core electrons [20]. The optical absorption spectrum is obtained by solving the Casida equations [21] under the Tamm-Dancoff approximation [22, 23]. The WOT-SRSH eigenvalues were used in the solution of the Casida equations and the TDDFT kernel is constructed using the WOT-SRSH parameters, see Ref. [24] for a detailed discussion of the equations. The effect of SOC is explicitly included.

C. Optical Absorption Spectra and *GW* Calculations

Many-body perturbation theory (MBPT) calculations, specifically single-shot G_0W_0 calculations to approximate the electron self-energy and obtain corrected bandstructures, as well as solutions to the Bethe-Salpeter Equation

(BSE) for optical absorption spectra, are carried out using the `BerkeleyGW` software package.

The effects of SOC are included either explicitly or perturbatively in all MBPT calculations. Frequency dependence in the dielectric function is included approximately via the Godby-Needs plasmon pole model (PPM) [25, 26], which has been shown to reproduce the computed bands gaps of full-frequency integration at reduced cost [27]. The static remainder approximation to Σ [28] is also used in order to obtain faster convergence with respect to the number of unoccupied bands. Convergence parameters, especially the number of bands used to construct ϵ_∞ and Σ, the energy cutoff in the construction of ϵ_∞, the size of the k- and q-grids being used, and the number of valence and conduction states used to calculate absorption spectra are taken from Ref. [1].

Also in line with Ref. [1], optical absorption calculations are carried out using the momentum operator, thus neglecting the contribution from the non-local part of the pseudopotential to the dipole transition matrix elements. This approximation has been shown to be valid for $Cs_2AgBiBr_6$ and it results in a significant computational speedup. Additionally, due to the increased cost of hybrid functional calculations, especially when attempting to obtain many unoccupied band or to solve for many $\boldsymbol{k}$-points, the optical spectra labeled G_0W_0-BSE@WOTSRSH in Fig. 4 of the main text was computed using WOT-SRSH eigenvalues with the wavefunctions and dielectric screening needed to solve the BSE obtained from PBE.

Specifics on the parameters used in the GW-BSE calculations can be found in Table II. Two variations of MBPT calculations are performed for $Cs_2AgBiBr_6$. The first is G_0W_0-BSE calculations using PBE. Convergence parameters for this case were taken directly from Ref. [1]. The dielectric screening and wavefunctions from these calculations were also used to perform a second optical absorption spectrum calculation using the eigenvalues obtained from the WOT-SRSH functional. In these calculations, SOC effects are considered explicitly. The second is a standard G_0W_0 calculation performed on top of the WOT-SRSH functional. Because of limitations of version 3.0 of `BerkeleyGW`, the self energy could not be computed with a hybrid starting point and SOC effects simultaneously. Therefore, we added in SOC effects perturbatively with splittings obtained at the WOT-SRSH level. This approximation has been shown to cause minimal error in semiconductors and insulators [29], but due to the large band splitting in $Cs_2AgTlBr_6$, there could be increase error in fully capturing the effects of SOC. Additionally, due to the increased cost of WOT-SRSH relative to a semi-local functional like PBE, the convergence parameters had to be reduced as seen in Table II.

A similar workflow (without the final self-energy calculation) is also carried out to compute the static RPA dielectric constant ϵ_∞^{-1} for $Cs_2AgTlBr_6$. In this case, while the PBE0 hybrid functional is used, because only the dielectric function needed to be calculated SOC effects were able to be handled explicitly. Moreover, they are found to have a very minimal impact, $\sim 1\%$, on the value of ϵ_∞^{-1}.

Compound	Method	Functional	SOC	N_{bands}	ϵ Cutoff (Ry)	k-grid (coarse)	k-grid (fine)	N_v	N_c	Broadening (eV)
$Cs_2AgBiBr_6$	BSE	PBE	Explicit	600	10	$4\times4\times4$	$12\times12\times12$	16	8	0.1
	G_0W_0	WOT-SRSH	Perturbative	640	30	$2\times2\times2$				
	TDDFT	WOT-SRSH	Explicit	–	22	–	$6\times6\times6$	16	8	0.1
$Cs_2AgSbBr_6$	G_0W_0	WOT-SRSH	Perturbative	640	30	$2\times2\times2$				
$Cs_2AgBiCl_6$	G_0W_0	WOT-SRSH	Perturbative	640	30	$2\times2\times2$				
$Cs_2AgSbCl_6$	G_0W_0	WOT-SRSH	Perturbative	640	30	$2\times2\times2$				
$Cs_2AgTlBr_6$	G_0W_0	PBE0	Explicit	300	10	$2\times2\times2$				
	G_0W_0	WOT-SRSH	Perturbative	640	30	$2\times2\times2$				

TABLE II. Convergence data for GW-BSE and TDDFT calculations.

II. CHECKING VARIANCE IN TUNING PARAMETERS

In Figure SI 1 we check the variance in γ as a function of of different α. In SI 2, we check to see if using different pseudo potentials has an effect on the value of γ. We find, as explained in the main text, γ changes with α, but the pseudopotential has a negligible effects on the tuned value of γ.

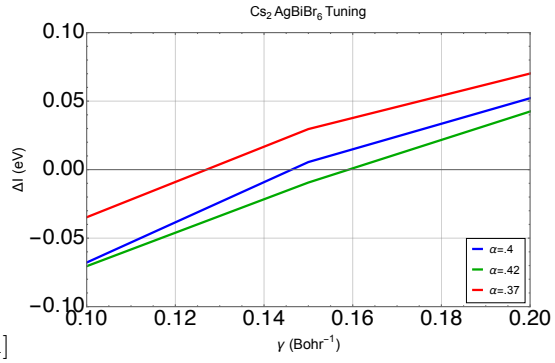

[SI 1]

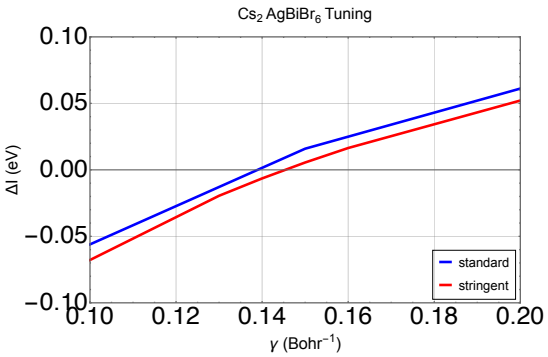

[SI 2]

FIG. 1. SI 1: α, γ tuning plot for $Cs_2AgSbBr_6$, for varying values of α. As expected varying α yields different γ. SI 2: Here we compare whether different pseudopotential (stringent vs standard fully relativistic) affect the tuning parameters. We find negligible effects on the value of γ.

[1] R. Biega, M. R. Filip, L. Leppert, and J. B. Neaton, J. Phys. Chem. Lett. **12**, 2057–2063 (2021).
[2] M. S. Hybertsen and S. G. Louie, Phys. Rev. Lett. **55**, 1418–1421 (1985).
[3] M. S. Hybertsen and S. G. Louie, Phys. Rev. B **34**, 5390–5413 (1986).
[4] J. Deslippe, G. Samsonidze, D. A. Strubbe, M. Jain, M. L. Cohen, and S. G. Louie, Comput. Phys. Commun. **183**, 1269–1289 (2012).
[5] M. J. van Setten, M. Giantomassi, E. Bousquet, M. J. Verstraete, D. R. Hamann, X. Gonze, and G. M. Rignanese, Comput. Phys. Commun. **226**, 39–54 (2018).
[6] M. Rohlfing, P. Krüger, and J. Pollmann, Phys. Rev. Lett. **75**, 3489–3492 (1995).
[7] W. Luo, S. Ismail-Beigi, M. L. Cohen, and S. G. Louie, Phys. Rev. B **66**, 195215 (2002).
[8] M. L. Tiago, S. Ismail-Beigi, and S. G. Louie, Phys. Rev. B **69**, 125212 (2004).
[9] A. Fleszar and W. Hanke, Phys. Rev. B **71**, 045207 (2005).
[10] J. Wiktor, I. Reshetnyak, F. Ambrosio, and A. Pasquarello, Phys. Rev. Materials **1**, 022401 (2017).
[11] J. P. Perdew, K. Burke, and M. Ernzerhof, Phys. Rev. Lett. **77**, 3865–3868 (1996).
[12] J. P. Perdew, M. Ernzerhof, and K. Burke, J. Chem. Phys. **105**, 9982–9985 (1996).
[13] L. Leppert, T. Rangel, and J. B. Neaton, Phys. Rev. Materials **3**, 103803 (2019).
[14] A. A. Mostofi, J. R. Yates, G. Pizzi, Y. Lee, I. Souza, D. Vanderbilt, and N. Marzari, Comput. Phys. Commun. **185**, 2309–2310 (2014).
[15] P. Giannozzi, S. Baroni, N. Bonini, M. Calandra, R. Car, C. Cavazzoni, D. Ceresoli, G. L Chiarotti, M. Cococcioni, I. Dabo, *et al.*, J. Phys.: Condens. Matter **21**, 395502 (2009).
[16] P Giannozzi, O Andreussi, T Brumme, O Bunau, M Buongiorno Nardelli, M Calandra, R Car, C Cavazzoni, D Ceresoli, M Cococcioni, *et al.*, J. Phys.: Condens. Matter **29**, 465901 (2017).
[17] P. Giannozzi, O. Baseggio, P. Bonfà, D. Brunato, R. Car, I. Carnimeo, C. Cavazzoni, S. de Gironcoli, P. Delugas, F. Ferrari Ruffino, *et al.*, J. Chem. Phys. **152**, 154105 (2020).
[18] D. Wing, G. Ohad, J. B. Haber, M. R. Filip, S. E. Gant, J. B. Neaton, and L. Kronik, PNAS **118**, e2104556118 (2021).
[19] G. Kresse and J. Furthmüller, Phys. Rev. B **54**, 11169–11186 (1996).
[20] G. Kresse and D. Joubert, Phys. Rev. B **59**, 1758–1775 (1999).
[21] M. E. Casida, in *Recent Advances in Density Functional Methods Part I*, edited by D. P. Chong (World Scientific, Singapore, 1995) Chap. 5, pp. 155–192.
[22] S. Hirata and M. Head-Gordon, Chem. Phys. Lett. **314**, 291–299 (1999).
[23] Carsten A Ullrich, *Time-dependent density-functional theory: concepts and applications* (OUP Oxford, 2011).
[24] S. Refaely-Abramson, M. Jain, S. Sharifzadeh, J. B. Neaton, and L. Kronik, Phys. Rev. B **92**, 081204 (2015).
[25] R. W. Godby and R. J. Needs, Phys. Rev. Lett. **62**, 1169–1172 (1989).
[26] A. Oschlies, R. W. Godby, and R. J. Needs, Phys. Rev. B **51**, 1527–1535 (1995).
[27] Paul Larson, Marc Dvorak, and Zhigang Wu, Phys. Rev. B **88**, 125205 (2013).
[28] J. Deslippe, G. Samsonidze, M. Jain, M. L. Cohen, and S. G. Louie, Phys. Rev. B **87**, 165124 (2013).
[29] S. E. Gant, J. B. Haber, M. R. Filip, F. Sagredo, D. Wing, G. Ohad, L. Kronik, and J. B. Neaton, Phys. Rev. Materials **6**, 053802 (2022).